

# PCCP

Accepted Manuscript



This is an *Accepted Manuscript*, which has been through the Royal Society of Chemistry peer review process and has been accepted for publication.

*Accepted Manuscripts* are published online shortly after acceptance, before technical editing, formatting and proof reading. Using this free service, authors can make their results available to the community, in citable form, before we publish the edited article. We will replace this *Accepted Manuscript* with the edited and formatted *Advance Article* as soon as it is available.

You can find more information about *Accepted Manuscripts* in the [Information for Authors](#).

Please note that technical editing may introduce minor changes to the text and/or graphics, which may alter content. The journal's standard [Terms & Conditions](#) and the [Ethical guidelines](#) still apply. In no event shall the Royal Society of Chemistry be held responsible for any errors or omissions in this *Accepted Manuscript* or any consequences arising from the use of any information it contains.

Spin-crossover in  
phenylazopyridine-functionalized Ni-porphyrin:  
*trans-cis* isomerization triggered by  $\pi$ - $\pi$   
interactions

Gerard Alcover-Fortuny,<sup>a</sup> Coen de Graaf<sup>f\*a,b</sup> and Rosa Caballol<sup>a</sup>

<sup>a</sup>Departament de Química Física i Inorgànica,  
Universitat Rovira i Virgili, Marcel·lí Domingo s/n,  
43007 Tarragona, Spain. E-mail: coen.degraaf@urv.cat

<sup>b</sup>Institució Catalana de Recerca i Estudis Avançats (ICREA)  
Passeig Lluís Companys 23, 08010 Barcelona, Spain

October 29, 2014

### Abstract

Reversible, room-temperature light-induced spin-crossover has been reported in a Ni-porphyrin functionalized with a phenylazopyridine (PAPy) ligand (Venkataramani *et al.*, Science **2011**, 331, 445). Upon light irradiation (500 nm), the azopyridine moiety induces a change in the Ni(II) coordination sphere from square planar ( $n = 4$ ) to square pyramid ( $n = 5$ ), leading to a change in the total spin of the molecule from  $S = 0$  to  $S = 1$ . The *trans-cis* isomerization in the azopyridine ligand has been proposed to trigger the spin-crossover effect. However, the radiation used to induce the HS state is about 135 nm red-shifted with respect to the radiation used for *trans-cis* isomerizations of the N=N double bond in other compounds. To elucidate the light-induced spin-crossover mechanism for this Ni(II) compound, a combined DFT/CASSCF/CASPT2 study has been performed to determine the most stable *cis* and *trans* conformers with  $n=4$  or  $n=5$ , and to characterize the excitation that triggers the SCO process.  $\pi - \pi$  interactions between porphyrin and PAPy are shown to play an essential role in the spin crossover.

## 1 Introduction

Many first row transition metal complexes present fascinating magnetic properties due to the presence of unpaired electrons in the 3d-shell. Transition metal ions with  $d^4$  to  $d^7$  electronic configurations are highly interesting because high-spin and low-spin configurations can be very close in energy depending on the nature of the coordinating ligands. Changes in the population of these configurations induced by external perturbations can lead to magnetic bistability when spin crossover (SCO) is accompanied by geometrical rearrangements in the complex. Particularly interesting for technical purposes are materials with SCO at room temperature [1]. These materials have attracted attention due to their potential application as sensors, optical switches, energy and information storage or energy transformation devices [2–5].

SCO can be induced by environmental changes, such as temperature, pressure, external magnetic fields or light. Among these possibilities, the latter variant is probably the most interesting one. The prototype SCO complex consists of a (quasi-)octahedral  $\text{FeN}_6$  core, where the nitrogen atom can be part of a monodentate or multidentate ligand [6–8]. At low temperatures, these complexes present a singlet ground state in most cases. The standard mechanism of light-induced SCO involves the excitation of an electron from the 3d orbitals of the Fe(II) ion into a higher lying orbital, for instance the  $\pi$  antibonding orbital of the coordinating ligand through a metal to ligand charge transfer (MLCT) excitation. This excitation is followed by a relaxation process through intersystem crossings and internal conversions to the metastable HS state [6, 9–21]. However, this is not the only way to induce SCO by light. The HS state can also be populated through photoisomerization reactions in the ligands (light-driven ligand-induced spin change, LD-LISC). When two isomers of a certain ligand exert a different ligand-field on the metal center, switching by light from one form to the other can invert the thermodynamic stability of the LS and HS states [22–24]. A more robust variant of this mechanism is based on a photoinduced change of the coordination number of the metal center. Isomerization can change an  $n$ -dentate ligand into an  $(n + 1)$ -dentate ligand or *vice-versa* [25, 26], and modify the ligand field strength in such a way that a spin change is induced.

Ni(II) complexes do not belong to the traditional class of SCO compounds.

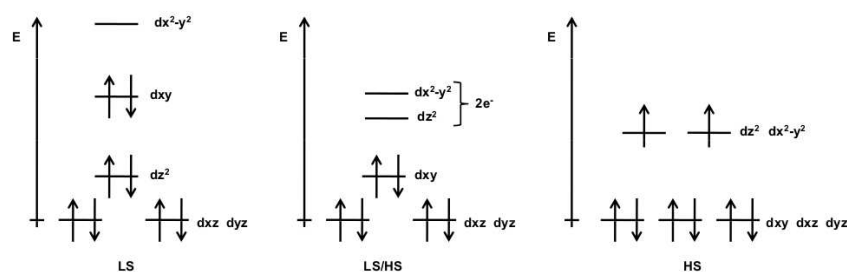


Figure 1: Electronic configurations of the 3d electrons of square-planar (left), square pyramidal (middle), and octahedral (right) Ni(II) complexes. Orbital energies are relative to the  $3d_{xz}$ ,  $3d_{yz}$  energy.

The sixfold, quasi-octahedral coordination mode strongly favors an  $S=1$  spin coupling of the  $3d^8$  configuration and complexes with square-planar (sqp) four-fold coordination usually have an  $S=0$  spin state. Square pyramidal (spy) pentacoordinated complexes can be found in both LS and HS states, but only recently a *classical* SCO system with a pentacoordinated Ni(II) has been identified [27]. In square-planar Ni(II)  $n=4$  complexes, the absence of axial ligands stabilizes the  $3d_{z^2}$  orbital with respect to the  $3d_{x^2-y^2}$  one. The  $3d_{xy}$ ,  $3d_{xz}$  and  $3d_{yz}$  are also more stable than the  $3d_{x^2-y^2}$  orbital, causing the pairing of all eight metal electrons and these complexes have singlet ground state, as shown in Fig. 1 on the left. On the other extreme, (quasi-)octahedral  $n=6$  complexes have (nearly-)degenerate  $3d_{z^2}$  and  $3d_{x^2-y^2}$  orbitals, favoring singly occupancy and therefore a triplet ground state ( $S=1$ ), see Fig. 1 on the right [28]. Square pyramidal  $n=5$  Ni(II) complexes can be either high-spin or low-spin depending on the nature of the axial ligand. In comparison to the square-planar coordination, the axial ligand stabilizes the  $3d_{xy}$  and  $3d_{x^2-y^2}$  orbitals with respect to the orbitals with a  $z$ -component. Depending on the gap between the  $3d_{z^2}$  and  $3d_{x^2-y^2}$  orbitals, the electrons occupy the  $3d_{z^2}$  orbital to form a  $S=0$  state or both orbitals are singly occupied leading to an  $S=1$  state, see Fig. 1 middle.

Transition metal (TM) porphyrins are planar structures that can easily incorporate axial ligands and therefore are good candidates for LD-LISC processes guided by changes in the coordination of the TM. Recently, room-temperature SCO has been reported for Ni-tetrakis(pentafluorophenyl)porphyrin (NiTPP)

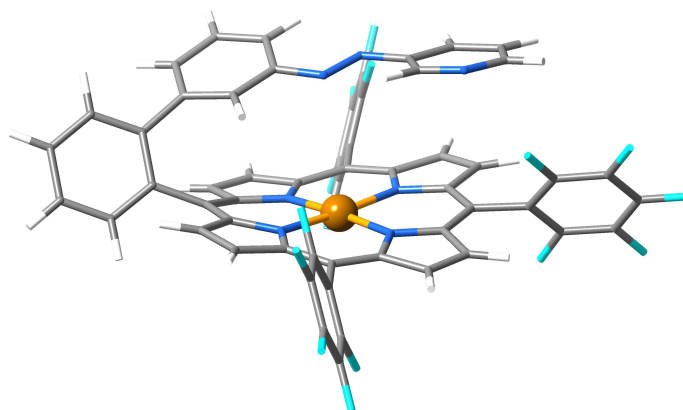


Figure 2: Ni-tetrakis(pentafluorophenyl)porphyrin with a phenylazopyridine functionalized axial arm (NiTPP-PAPy).

functionalized with a phenylazopyridine (PAPy) arm [26], see Fig. 2. Under standard conditions, the NiTPP-PAPy complex is low-spin ( $S=0$ ) and NMR experiments, among other characterization techniques, indicate a tetracoordinated Ni(II) in a square planar geometry with a *trans* configuration of the PAPy arm. Upon irradiation at 500 nm, the compound becomes paramagnetic and rearranges to a pentacoordinated complex where the pyridine moiety coordinates axially to Ni(II), which becomes high-spin. The SCO process in this Ni-porphyrin is reversible upon irradiation at 435 nm, while the thermal back reaction is very slow.

The authors interpret that the SCO process is triggered by the *trans-cis* isomerisation of the N=N bond of the PAPy arm. Irradiation at 500 nm induces a  $\pi-\pi^*$  excitation on the azo group and the PAPy arm evolves to the *cis* isomer. This orients the non-bonding electron pair of pyridine nitrogen perpendicularly to the Ni-porphyrin plane, making possible the coordination of the arm to Ni. The assignment of the paramagnetic product as a pentacoordinated Ni ion with the PAPy arm in the *cis* form was based on NMR Overhauser experiments, indicating that the Ni-H distance of the two hydrogens adjacent to the nitrogen of the pyridine ring is identical for both H atoms and significantly smaller than in the initial complex. The pentacoordination of the Ni(II) ion induces a spin change to  $S=1$ , further stabilized by the electron withdrawing pentafluorophenyl

groups attached to the porphyrin ring that lower the energy of the  $3d_{x^2-y^2}$  orbital and decrease the gap with the  $3d_{z^2}$  orbital (see Fig. 1, middle) [28]. Upon irradiation with visible light (435 nm) or by heating the sample, the PAPy arm recovers the initial *trans* conformation and the pyridine group dissociates from Ni(II), which turns back to its initial low-spin configuration.

However, this description of the LD-LISC leaves a few points open to discussion. The most important one is the fact that the irradiation used to induce the HS state is significantly red-shifted ( $\sim 135$  nm) with respect to the wavelength normally used for *cis-trans* isomerizations of N=N double bonds. In fact, the 500 nm irradiation used in the experiments is typical for the Q band absorption of porphyrins. A second point is related to the indirect characterization of the *cis* isomer of the arm in the paramagnetic product, which is based on measurements on the diamagnetic Zn-analogue of the NiTPP-PAPy complex. Furthermore, the PBE functional used in the density functional theory (DFT) geometry optimizations may not be the most appropriate choice given the large  $\pi$ -systems of the porphyrin ring and the PAPy arm. The interaction between  $\pi$ -systems is in general not accurately described with standard GGA functionals.

Light induced SCO in simpler Ni(II) porphyrins in basic solvents as pyridine has been observed before. The mechanism is well established and goes through the 500 nm excitation in the Q band from the LS ground state ( $S_0$ ) to an excited singlet state ( $S_2$ ). This transition involves  $\pi$  and  $\pi^*$  orbitals of the porphyrin system. The  $S_2$  state relaxes via an intersystem crossing directly to  $T_1$  or via  $S_1$  through internal conversion followed by an intersystem crossing as schematically depicted in Fig. 3. A solvent molecule is then axially coordinated to the Ni(II) and the pentacoordinated species relaxes to the  $T_0$  state [29–32].

The aim of the present work is to get more insight in the details of LD-LISC mechanism of NiTPP-PAPy. We clarify the origin of the 500 nm irradiation that triggers the SCO and discuss the geometries and relative stabilities of several *cis* and *trans* isomers of the complex in LS and HS configurations. For this purpose, we apply DFT/M06-2X calculations to optimize the geometries combined with CASPT2 calculations for accurate energetics.

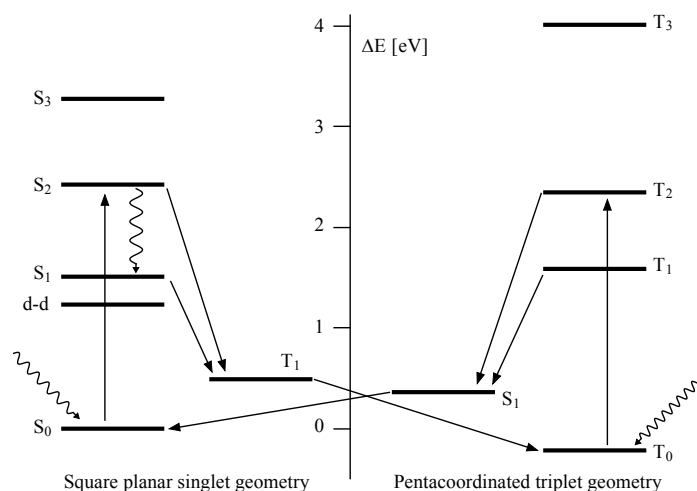


Figure 3: Schematic representation of the SCO mechanism in Ni-porphyrin complexes.

## 2 Computational information

Dispersion forces are poorly described with standard DFT schemes. Since the  $\pi$ - $\pi$  interactions between porphyrin and PAPy arm can be determinant for the relative stabilities of the different conformers, we compare standard BP86 [33, 34] results with those obtained with the dispersion corrected functional M06-2X [35]. The DFT calculations are performed with the Gaussian09 package [36]. A triple zeta valence + polarization (TZVP) [37] basis set was used for the Ni(II) ion and basis sets of split-valence + polarization (SVP) quality [38] for the rest of the atoms. The optimized geometries were characterized as minima on the potential energy surface by frequency calculations. Solvent effects were included by means of the COSMO model [39, 40] using the dielectric constant of dimethyl sulfoxide ( $\epsilon=46.7$ ) to mimic the experimental conditions.

To address the energetics of the ground and excited states in the different isomers, we apply multiconfigurational wave function based methods. Although computationally much more demanding, they provide accurate, well-balanced descriptions of ground and excited states of different spin multiplicity in TM complexes. Among the different options, we opt for a standard strategy con-

sisting of the complete active space self-consistent field (CASSCF) approach followed by a second-order perturbation (CASPT2) treatment of the remaining electron correlation effects. Calculations are performed with the Molcas 7 package [41, 42]. A Cholesky decomposition of the two-electron integrals is used to reduce the computational cost. The basis sets centered on the different atoms are of the atomic natural orbitals type (ANO-RCC)[43–45]. Apart from being advantageous to recover the maximum of the correlation energy, these basis sets are also optimized for scalar relativistic effects and core correlation. The most relevant atoms in the NiTPP-PAPy and Ni-porphyrin systems (Ni and N) are described with a TZVP basis set, while the more peripheral atoms (C, F and H) have a basis set of double-zeta quality. In the PAPy arm, the basis set for carbon atoms is also of TZVP quality.

The size of the active space to construct the reference CASSCF wave function for CASPT2 is critical to obtain reliable results. The standard active space in the CASSCF calculations on the complexes with Ni (NiTPP-PAPy, and Ni-porphyrin + pyridine) contains 10 electrons distributed in all possible ways over eleven orbitals, [10,11]-CASSCF. Ten of the active orbitals are localized on Ni. From these, five orbitals show mainly contributions from the Ni-3d basis functions and the other five are built from more diffuse d-functions. This double d-shell is essential to account for the large correlation effects in the crowded Ni-d shell. The remaining active orbital is essentially localized on the N-atoms of the porphyrin that coordinate to Ni, describing the lone-pairs interacting with the electrons in the  $3d_{x^2-y^2}$  orbital of Ni. This active space suffices to calculate the relative stability of the fundamental singlet and triplet states in the tetra- and pentacoordinated species. For the study of the vertical excitation energies in NiTPP-PAPy a [8,10]-CASSCF wave function is considered. The nature of the active orbitals will be specified in the presentation of the results. CASSCF calculations on the PAPy arm were done with an active space of 12 electrons and 9 orbitals ( $\pi$ ,  $\pi^*$ , and N lone pair orbitals), further details on the shape of the orbitals will be given when discussing the vertical spectrum. The absorption spectrum of Ni-porphyrin was calculated with an active space of 14 electrons and 16 orbitals.

Table 1: BP86 and M06-2X Ni-N<sub>pyridine</sub> distances and relative energies for several conformations of PAPy-NiTPP. Square planar (sqp) conformations are singlet and have fourfold Ni coordination. Square pyramid (spy) conformers are triplet and pentacoordinated.

Configuration	Ni-N <sub>pyridine</sub> distance (Å)		Relative energy (eV)	
	BP86	M06-2X	BP86	M06-2X
<i>trans</i> -sqp	6.99	4.36	-0.81	0.42
<i>trans</i> -sqp open	12.34	11.52	-0.81	0.72
<i>cis</i> -sqp	4.30	2.62	-0.25	0.91
<i>cis</i> -sqp open	9.44	9.39	-0.23	1.32
<i>trans</i> -spy	2.08	2.17	0.15	0.28
<i>cis</i> -spy	2.08	2.16	0.00	0.00

### 3 Results and discussion

#### 3.1 Conformational analysis

To rationalize the SCO process, Venkataramani *et al.* [26] performed DFT calculations on a series of potentially suitable molecular structures. They used the PBE functional [46, 47] and found several minima for *cis* and *trans* tetra-coordinated and pentacoordinated NiTPP-PAPy. For this last coordination only a stable structure was found with the *cis* configuration of the PAPy arm. As explained in the computational information, the present work compares the optimization process by means of the BP86 functional, which is supposed to give similar results as PBE, to those obtained with dispersion corrected functionals. In this way we can access the importance of the  $\pi$ - $\pi$  interactions and locate the minimum structure of the pentacoordinated complex with the PAPy arm in *trans*.

Table 1 reports M06-2X relative energies and nickel-nitrogen distance, d(Ni-N<sub>pyridine</sub>), of the different minima found for both *cis* and *trans* PAPy arm configurations. The BP86 optimized metal-nitrogen distance and relative energies are also reported for comparison. All sqp structures have a singlet ground state and the spy complexes are triplet. The M06-2X optimized structures are repre-

sented in Fig. 4. The *trans*-sqp conformer is the most stable singlet structure, and the pentacoordinated *cis*-spy  $S = 1$  structure is the absolute minimum of the whole set. As a general feature, the axial coordination slightly enlarges the distance between nickel and the porphyrin-nitrogens, from 1.99 to 2.06 Å. This lengthening of the bond can be easily related to the single occupancy of the  $3d_{x^2-y^2}$  orbital (of Ni-N antibonding character) in the HS state, being empty in the LS state. Geometry optimizations of *trans*-sqp and *cis*-spy with a larger basis set (TZVP on all atoms), and with the B97D functional (Grimme dispersion corrected) give practically the same results; most distances and angles do not differ by more than 0.1 Å and 5 degrees in both cases. The largest change is observed in the Ni-N<sub>pyridine</sub> distance in *trans*-sqp. The 4.36 Å predicted by the M06-2X functional changes to 4.21 Å with B97D. This 0.15 Å reduction reflects the relatively flat potential of the PAPy arm when it is not coordinated to the Ni atom.

The role of dispersion forces is particularly noticeable in the tetracoordinated *trans*-sqp minimum, where the pyridine ring is parallel to the porphyrin unit and  $\pi$ - $\pi$  interaction is important. The distance between Ni and the N of the pyridine is shortened by 2.6 Å when the dispersion is included in the calculation. The influence of long-range interactions is also evident in the *cis*-sqp conformer, where the relatively short Ni-N<sub>pyridine</sub> distance suggests an incipient pentacoordination, albeit with a singlet ground state. In this case the nitrogen lone pair is not conveniently oriented to Ni(II), since the angle between the pyridine and porphyrin planes is 79°. Hence, the gap between the  $3d_{z^2}$  and  $3d_{x^2-y^2}$  orbitals stays large and the singlet remains the ground state.

However, the most important consequence of including long-range interactions in the calculations of the present system is the strong stabilization of the *trans*-spy triplet. BP86 predicts a very high energy (0.96 eV) for this pentacoordinated structure with respect to the tetracoordinated *trans* conformers, while M06-2X predicts it to be 0.14 eV more stable than *trans*-sqp. Beside being close in energy, the square pyramid *cis* and *trans* isomers have also similar Ni-N<sub>pyridine</sub> distances, 2.16-2.17 Å, compatible with the experimentally estimated value of 2.1 Å. Recalling that the *cis* configuration of the product was assigned from Nuclear Overhauser experiments on a diamagnetic Zn analog, we conclude

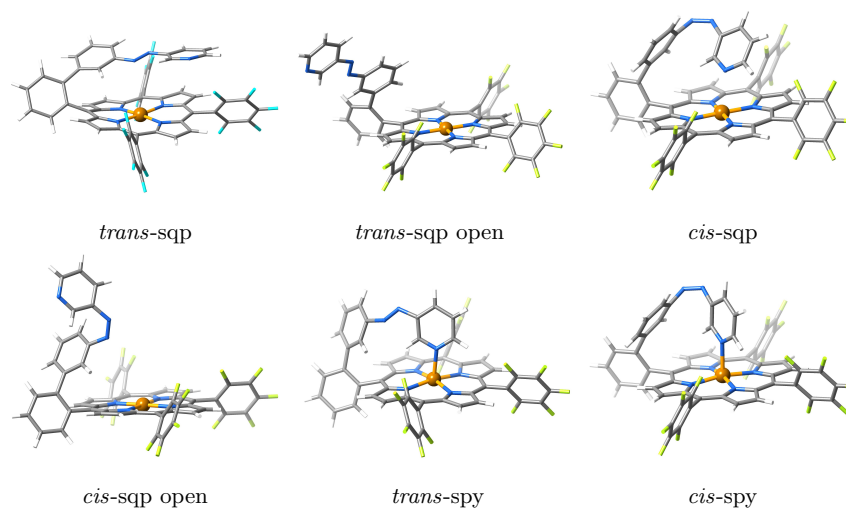


Figure 4: M06-2X geometries of the NiTPP-PAPy conformers listed in Table 1.

that the *trans* structure cannot be excluded yet as a possible candidate of the pentacoordinated paramagnetic product and that alternative mechanisms not involving azopyridine *trans-cis* isomerization as the key step of the SCO process should not be completely discarded.

Finally, we mention that the differences between the geometry optimizations in vacuum and those with solvent effects through the PCM model lead to virtually the same results. Neither the energies, nor the geometrical parameters show any significant changes when the complex is treated in a DSMO solvent. All the results reported below are obtained in vacuum.

### 3.2 Axial coordination in *cis* and *trans* NiTPP-PAPy

The standard active space for an accurate determination of the relative stability of different spin states in (quasi-)octahedral TM-3d<sup>*n*</sup> ( $n \geq 5$ ) complexes consists of ( $n + 4$ )-electrons and 12 orbitals [48]. In addition to the TM-3d orbitals and the extra set of *d*-orbitals to account for the double shell effect, one should also include the two ligand- $\sigma$  orbitals of  $e_g$ -like symmetry in the active space. However, in the present case this choice necessarily leads to an unbalanced description of the four- and five-coordinated species. The in-plane  $\sigma$ -orbital of the N<sub>porph</sub> atoms is easily included in the active space for both species, but the

second  $\sigma$  orbital corresponding to the axial ligand can only be included in the five-coordinated complexes. The corresponding orbital in the four-coordinated species is the lone pair orbital of the N atom on the pyridine ring, which in itself contributes very little to the electron correlation, and hence, does not stay in the active space. Therefore, we calculate the relative stability of the singlet and triplet state of the different NiTPP-PAPy species with a [10-11]-CASSCF wave function. The stability of the results was checked by comparing the singlet-triplet splitting of different five-coordinated species to the results obtained with the [12,12]-CASSCF calculations. The shape of the active orbitals is given in the Supporting Information. CASSCF single point calculations were performed using the DFT optimized structures of most stable conformers: *trans*-sqp, *cis*-spy and *trans*-spy.

The relative energies listed in Table 2 indicate that both CASSCF and CASPT2 correctly predict a triplet ground state for the pentacoordinated conformers. However, CASSCF fails to establish a singlet ground state for the four-coordinated sqp complex, which is repaired by including dynamic correlation through CASPT2. The results with the [12,12] active space are only slightly different to those obtained with the smaller active space. Interestingly enough, CASPT2 places the triplet of the *trans*-spy isomer energetically close to the initial singlet state of the square planar conformation, which does not discard the possibility of a SCO process without *trans-cis* isomerization.

To further settle the question about the mechanism, we have calculated triplet energies along the dissociation path of the PAPy arm from the Ni ion. This provides information about the thermal stability of the light induced pentacoordinated product in the *cis* and *trans* forms. The points along the scan were generated with M06-2X geometry optimizations fixing the Ni-N<sub>py</sub> distances at different values. As shown in Fig. 5, the release of the pyridine group of the PAPy arm in the *trans*-spy form is nearly barrierless, while a steep rise in the energy is observed when the Ni-N distance is increased in the *cis*-spy isomer. The energy along this path reaches a maximum at  $d(\text{Ni-N}_{\text{azo}}) = 3.3 \text{ \AA}$ , where it is 0.84 eV higher than the triplet of the pentacoordinated *cis* isomer. This means that a hypothetical triplet pentacoordinated NiTPP-PAPy in *trans* form will release the axial ligand very rapidly at room temperature and that this

Table 2: CASSCF and CASPT2 relative energies in eV of singlet and triplet states of *trans*-sqp, *cis*-spy and *trans*-spy.

	Spin	[10,11]		[12,12]
		CASSCF	CASPT2	CASSCF
<i>trans</i> -sqp	singlet	0.94	0.26	–
	triplet	0.70	0.39	–
<i>cis</i> -spy	singlet	1.34	1.07	1.39
	triplet	0.00	0.00	0.00
<i>trans</i> -spy	singlet	1.67	1.32	1.73
	triplet	0.36	0.29	0.36

process is slow for the *cis* form. Finally, we mention that the relative stability of the singlet *trans*-sqp and the triplet *cis*-spy states is opposite to what may be expected. This can at least partially be ascribed to the limited basis set that we use in our calculation. It is well-known that larger basis sets (especially on the metal) are needed to obtain correct high-spin/low-spin energy differences in spin crossover processes [48–50]. However, such lowering of the singlet state(s) will not affect any of the arguments discussed above, and hence, the only plausible mechanism to explain the LD-LISC in this compound is via *trans-cis* isomerization. However, note that the 500 nm irradiation does not directly cause a  $\pi_{azo} \rightarrow \pi_{azo}^*$  transition in PAPy and similar systems and the nature of the excitation causing the isomerization needs further clarification.

### 3.3 Vertical excitation energies of PAPy

In order to locate the  $\pi_{azo} \rightarrow \pi_{azo}^*$  excitation in the absorption spectrum and to characterize the 500 nm band of the NiTPP-PAPy complex, we first calculated the vertical excitation spectrum of the PAPy arm. The minimal active space to correctly study the vertical excitation spectrum of the PAPy arm should contain the  $\pi$  and  $\pi^*$  orbitals of the N=N bond and the lone pair orbitals ( $n_{azo}$ ) of the nitrogen atoms, extended with two pairs of  $\pi$  and  $\pi^*$  orbitals of the phenyl and pyridine side groups ( $\pi_{side}$  and  $\pi_{side}^*$ ), and the lone pair orbital of the pyridine nitrogen. This active space with 12 electrons and 9 orbitals was used

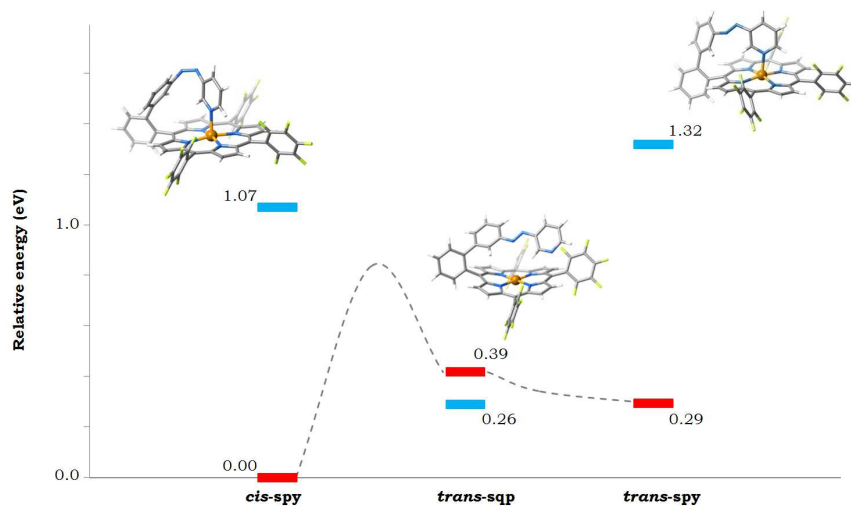


Figure 5: CASPT2 energies of the singlet (blue) and triplet (red) states of NiTPP-PAPy. The dashed lines connect the triplet state of the tetracoordinated complex (middle) to the pentacoordinated species *cis-spy* (left) and *trans-spy* (right).

to generate the reference wave function for the subsequent CASPT2 calculations. Active orbitals are graphically represented in the Supporting Information and the results are summarized in Table 3.

The effect of electron correlation on the excitation energies is large, especially for the  $\pi_{side} \rightarrow \pi_{azo}^*$  transitions. The very high CASSCF energy of these states ( $\sim 6$  eV) is lowered by approximately 2.5 eV by the CASPT2 treatment of the electron correlation. The CASPT2 transition energies are in good agreement with the experimental values for all states. The most important features of the

Table 3: [9,12]-CASPT2 vertical excitation energies in eV of *trans* 3-phenylazopyridine (3-PAPy). Experimental values are given for comparison.

<i>trans</i> 3-PAPy	CASSCF	CASPT2	Oscillator strength	Exp. [51]
$n_{azo} \rightarrow \pi_{azo}^*$	3.15	2.75 (450 nm)	$6.22 \cdot 10^{-8}$	2.76
$\pi_{side} \rightarrow \pi_{azo}^*$	5.96	3.48 (356 nm)	0.32	3.91
$\pi_{azo} \rightarrow \pi_{azo}^*$	7.41	6.99 (177 nm)	0.28	

excitation spectrum are a low-lying  $n_{azo} \rightarrow \pi_{azo}^*$  excitation around 2.75 eV (450 nm) and a high intensity  $\pi_{side} \rightarrow \pi_{azo}^*$  transition appearing at 3.48 eV (356 nm). The lowest CASSCF root that involves  $\pi_{azo}$  and  $\pi_{azo}^*$  orbitals is located at an energy of 7.41 eV and CASPT2 lowers the transition energy to 6.99 eV (177 nm), much higher in energy than the reported 500 nm wavelength to induce SCO.

### 3.4 Vertical excitation energies of NiTPP-PAPy

An important question that remains to be answered is the nature of the 500 nm excitation used to induce the SCO in the NiTPP-PAPy complex. The CASPT2 results of the PAPy subsystem place the  $\pi \rightarrow \pi^*$  excitation at higher energies, in concordance with the findings in other azobenzene derivatives, but the interaction of the PAPy arm with the porphyrin system may shift the  $\pi \rightarrow \pi^*$  transition to lower energies as suggested by Venkataramani [26]. Hence, to obtain a complete description of the optical transitions of the NiTPP-PAPy system, the  $\pi$  system of the porphyrin ring should also be considered. The most basic description of the optical absorption of porphyrin systems involves at least four orbitals as established by numerous studies that go back to the original four-orbital model of Gouterman [52–54]. Adding these four orbitals ( $\pi_{porph}$ ) to the lone pair orbitals ( $n_{azo}$ ),  $\pi_{azo}$  and  $\pi_{azo}^*$  of the PAPy arm gives a [10,8]-CASSCF wave function. The shape of the 8 active orbitals is given in the Supporting Information. This active space does not describe any excited state involving the electrons in the Ni-3d orbitals, but the metal-centered excitations have a low oscillator strength and the charge transfer excitations appear at higher energy. Whereas the inclusion of the Ni-3d and 3d' orbitals is essential to obtain accurate estimates of the relative stability of the different species, this is rather unimportant for the vertical spin allowed excitations from the closed shell  $n = 4$  ground state.

Table 4 lists the lowest calculated transition energies and the corresponding oscillator strengths. The states are labeled according to the most important electron replacements involved in the excitation. The lowest two transitions have intermediate oscillator strength and can be associated to the Q bands observed around 523 nm in the experimental work. The  $\pi$  orbitals involved in

Table 4: [10,8]-CASPT2 vertical excitation energies in eV of *trans*-sqp NiTPP-PAPy. Experimental values are given for comparison.

<i>trans</i> NiTPP-PAPy	CASSCF	CASPT2	Oscillator strength	Exp.[26]
$\pi_{porph} \rightarrow \pi_{azo+porph}^*$	3.55	2.59 (478 nm)	$3.70 \cdot 10^{-2}$	523
$\bar{\pi}_{porph} \rightarrow \bar{\pi}_{azo+porph}^*$	3.57	2.65 (467 nm)	$5.60 \cdot 10^{-2}$	523
$n_{azo} \rightarrow \pi_{azo}^*$	3.60	3.23 (383 nm)	$9.00 \cdot 10^{-6}$	406
$n_{azo} \rightarrow \pi_{azo}^* / \pi_{porph} \rightarrow \pi_{azo}^*$	5.29	4.57 (271 nm)	$5.90 \cdot 10^{-4}$	322

these transitions are well localized on the porphyrin ring, but as is shown in Fig. 6 the  $\pi^*$  orbitals have a non-negligible contribution from the antibonding combination of the N-2p orbitals of the azo bond of the PAPy arm. Hence, the Q band is not simply a porphyrin centered excitation but also causes a certain degree of occupation of the  $\pi_{azo}^*$  orbital. This weakens the N=N bond and could very well trigger a *trans-cis* isomerization. It is interesting to compare these orbitals with those of the *trans*-sqp optimized geometry obtained with the BP86 functional (see Supporting Information). The PAPy arm is more separated from the porphyrin ring in this geometry and the orbitals are either pure  $\pi_{porph}^*$  or  $\pi_{azo}^*$ , without any mixing. This suggests a determinant role of the  $\pi - \pi$  interactions in this SCO mechanism, revealed by the M06-2X functional. The important shortening of the porphyrin-pyridine distance (Table 1) induces the delocalization and the subsequent possibility of populating the  $\pi^*$  orbital at lower energy.

Severe intruder state problems hinder the accurate description of the  $\pi_{azo} \rightarrow \pi_{azo}^*$  excitation in the large complex. However, the similarity of the SA-CASSCF excitation energy (7.25 eV) with the one obtained for the PAPy arm (see Sec. 3.3) situates the  $\pi_{azo} \rightarrow \pi_{azo}^*$  excitation in NiTPP-PAPy at significant higher energy than the 2.5 eV (500 nm) used in the experiments to induce the SCO.

While the Q band is well reproduced by our calculations, the experimental absorption spectrum of NiTPP-PAPy shows a Soret band of high intensity at 406 nm. At this region a  $n_{azo} \rightarrow \pi_{azo}^*$  excitation is found, but the low oscillator strength cannot explain the experimentally observed intense peak. Probably, this low intensity band is hidden by the optically allowed  $\pi_{porph} \rightarrow \pi_{porph}^*$

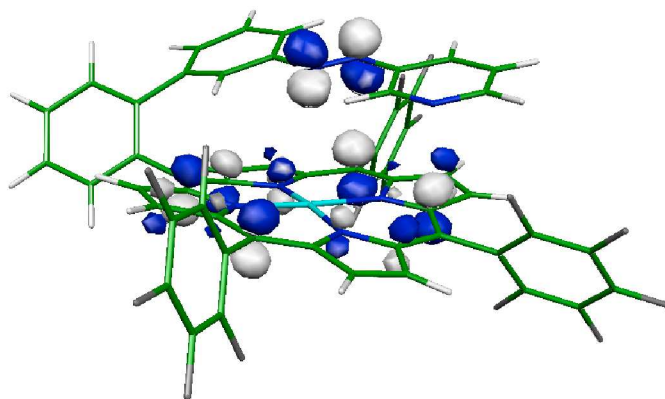


Figure 6: Graphical representation of the orbital that is occupied in the lowest two vertical excitations of NiTPP-PAPy.

excitations of the porphyrin moiety which cannot be reproduced with the present [10,8]-CAS [55].

### 3.5 Vertical excitation energies of Ni-porphyrin

Previous studies show that for an accurate description of the absorption spectrum of porphyrin and its derivatives, the basic Gouterman model is not good enough, and more orbitals have to be included in the active space of the CASSCF calculations. The "minimal" active space for correctly addressing the vertical spectrum of porphyrins consists of 8  $\pi$  and 6  $\pi^*$  orbitals. Hence, a complete account of the vertical absorption spectrum of NiTPP-PAPy requires a [20,18]-CAS (14 porphyrin orbitals,  $\pi$ ,  $\pi^*$  and two lone pair orbitals of the azo-group on the PAPy arm). This is clearly beyond the limits of CASSCF and the spectrum has to be calculated by parts. On the one hand, the 8 orbital and 10 electrons active space used in section 3.4 allows to calculate the Q band. On the other hand, an active space consisting of 8  $\pi$  and 6  $\pi^*$  orbitals of the porphyrin is used to characterize the Soret band, which is expected to be a  $\pi_{porph} \rightarrow \pi^*_{porph}$  excitation [55]. A [16,14]-CASPT2 is cumbersome for NiTPP-PAPy, and therefore, this calculation has been carried out on the Ni-porphyrin system (see Fig. 7). Ni-porphyrin presents  $D_{2h}$  point group symmetry. Two pairs of  $\pi$ - $\pi^*$  orbitals

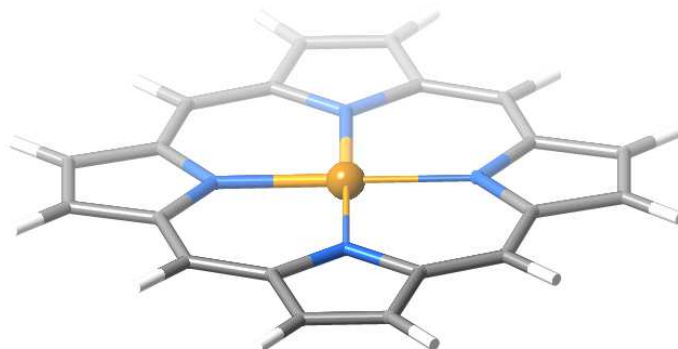


Figure 7: Ni-porphyrin model used to study the contribution of the porphyrin moiety to the absorption spectrum of NiTPP-PAPy.

Table 5: [16,14]-CASPT2 vertical excitation energies in eV of Ni-porphyrin.

State	CASSCF	CASPT2	Oscillator strength
$^1B_{2u}$	3.72	2.66 (465 nm)	$1.45 \cdot 10^{-2}$
$^1B_{3u}$	3.09	2.73 (453 nm)	$1.58 \cdot 10^{-2}$
$^1B_{2u}$	5.54	3.70 (335 nm)	1.18
$^1B_{3u}$	4.42	4.08 (303 nm)	0.22

with  $b_{2g}$  and  $b_{3g}$  characters, a pair of  $\pi$ - $\pi^*$  orbitals with  $a_u$  character and a set of 3  $\pi$  and 1  $\pi^*$  orbitals with  $b_{1u}$  character are taken to form the 14 orbitals active space. The shape of the active orbitals is shown in the Supporting Information.

Table 5 lists the four lowest  $\pi \rightarrow \pi^*$  excitations of Ni-porphyrin system. The most intense band is due to the transition to the second  $^1B_{2u}$  state and appears at 335 nm. The deviation respect to the experimental Soret band of the NiTPP-PAPy (406 nm) can be attributed to the geometrical differences between the whole system and the Ni-porphyrin model. Furthermore, the calculated oscillator strength for this excitation shows that this band is of high intensity compared to the bands obtained in section 3.4. One can conclude that for the NiTPP-PAPy spectrum, the Q band corresponds to  $\pi_{porph} \rightarrow \pi_{azo+porph}^*$  and the Soret band to  $\pi_{porph} \rightarrow \pi_{porph}^*$  excitations not relevant for the SCO mechanism.

## 4 Summary and Conclusion

Although the original proposal of a *trans-cis* isomerization of the N=N double bond induced by a  $\pi \rightarrow \pi^*$  excitation offers a plausible explanation for reversible room-temperature spin crossover observed in NiTPP-PAPy, the large red-shift of 150 nm of the excitation energy leaves some room for improvement. SCO in standard Ni-porphyrins is induced by a  $\pi - \pi^*$  excitation of 2.5 eV (500 nm) on the porphyrin ring. The same wave length was used in the experiments on NiTPP-PAPy and therefore we first investigated the possibility of SCO induced by a  $\pi - \pi^*$  excitation on the porphyrin ring without the need of a *trans-cis* isomerization. The inclusion of the effect of dispersion forces in the geometry optimization using the M06-2X functional leads to *cis* and *trans* isomers with four- and five-coordinated Ni ions in a relatively small energy window. Single point CASPT2 calculations on the optimized geometries predicts a near degeneracy for the low-spin state of the four-coordinated complex and the high-spin state of the five-coordinated complex with the PAPy arm in *trans* conformation. However, the absence of a barrier along the dissociation path of the PAPy arm in a hypothetical all-*trans* mechanism is incompatible with the experimental stability of the high-spin state. On the contrary, a significant barrier was found for the dissociation of the PAPy-arm in the *cis* conformation.

Subsequently, we used CASSCF/CASPT2 calculations to clarify the character of the excitation that induces the *trans-cis* isomerization at 500 nm. The  $\pi - \pi^*$  excitation on the azo group was found at very high energy and the excitation from the  $\pi$  orbitals of the six-membered rings bonded to the N=N group into the N=N  $\pi^*$  orbital occurs at 350 nm, also too high to be assigned to the experimental excitation. The CASPT2 results identify the 500 nm transition as an excitation involving a bonding  $\pi$  orbital of the porphyrin ring and an antibonding  $\pi^*$  orbital with important contributions from both the porphyrin system and the N=N group. The occupation of this anti-bonding orbital of mixed character weakens the N=N bond and leads to a *trans-cis* isomerization.

Hence, the combination of DFT and multiconfigurational wave function calculations is able to firmly establish the *trans-cis* isomerism in PAPy arm as mechanism for the spin crossover in NiTPP-PAPy. The structures obtained with DFT/M06-2X show that the arm is closer to the porphyrin ring than in

the structure without taking into account the dispersion. The character of the excitation that triggers the spin crossover is identified and involves the electron replacement from a bonding  $\pi$  orbital on the porphyrin to an antibonding orbital with contributions on the porphyrin and the azo group.

### Acknowledgments

Financial support has been provided by the Spanish Administration (Project CTQ2011-23140), the Generalitat de Catalunya (Projects 2014SGR199 and Xarxa d'R+D+I en Química Teòrica i Computacional, XRQTC) and the European Union (COST Actions CODECS CM1002 and ECOSTBio CM1305).

### Supporting information

Coordinates and total energies of the M06-2X optimized geometries of the NiTPP-PAPy conformers used in this study. Graphical representations of the active orbitals of NiTPP-PAPy, PAPy and Ni-porphyrin.

### References

- [1] A. Bleuzen, V. Marvaud, C. Mathonière, B. Sieklucka and M. Verdaguer, *Inorg. Chem.*, 2009, **48**, 3453.
- [2] O. Sato, *J. Photochem. Photobiol. C*, 2004, **5**, 203.
- [3] J.-F. Létard, P. Guionneau and L. Goux-Capes, *Spin crossover in Transition Metal Compounds III*, Springer-Verlag, Berlin, 2004, vol. 235, p. 221.
- [4] S. M. Aldoshin, *J. Photochem. Photobiol. A*, 2008, **200**, 19.
- [5] K. Szaciłowski, *Chem. Rev.*, 2008, **108**, 3481.
- [6] P. Gütllich, Y. Garcia and H. A. Goodwin, *Chem. Soc. Rev.*, 2000, **29**, 419.
- [7] J.-F. Létard, P. Guionneau, O. Nguyen, J. Sánchez Costa, S. Marcén, G. Chastanet, M. Marchivie and L. Goux-Capes, *Chem. Eur. J.*, 2005, **11**, 4582.
- [8] A. Hauser, C. Enachescu, L. M. Lawson Daku, A. Vargas and N. Amstutz, *Coord. Chem. Rev.*, 2006, **250**, 1642.
- [9] J. J. McGarvey and I. Lawthers, *J. Chem. Soc., Chem. Commun.*, 1982, 906.
- [10] S. Decurtins, P. Gütllich, C. P. Köhler, H. Spiering and A. Hauser, *Chem. Phys. Lett.*, 1984, **105**, 1.

- [11] A. Hauser, *J. Chem. Phys.*, 1991, **94**, 2741.
- [12] J. K. McCusker, K. N. Walda, R. C. Dunn, J. D. Simon, D. Magde and D. N. Hendrickson, *J. Am. Chem. Soc.*, 1993, **115**, 298.
- [13] P. Gütllich, A. Hauser and H. Spiering, *Angew. Chem. Int. Ed.*, 1994, **33**, 2024.
- [14] A. Hauser, *Spin crossover in Transition Metal Compounds I*, Springer-Verlag, Berlin, 2004, vol. 233, p. 49.
- [15] H. Ando, Y. Nakao, H. Sato and S. Sakaki, *J. Phys. Chem. A*, 2007, **111**, 5515.
- [16] A. L. Smeigh, M. Creelman, R. A. Mathies and J. K. McCusker, *J. Am. Chem. Soc.*, 2008, **130**, 14105.
- [17] A. Cannizzo, C. J. Milne, C. Consani, W. Gawelda, C. Bressler, F. van Mourik and M. Chergui, *Coord. Chem. Rev.*, 2010, **254**, 2677.
- [18] M. Chergui, *Dalton Trans.*, 2012, **41**, 13022.
- [19] N. Huse, T. K. Kim, L. Jamula, J. K. McCusker, F. M. F. de Groot and R. W. Schoenlein, *J. Am. Chem. Soc.*, 2010, **132**, 6809.
- [20] C. de Graaf and C. Sousa, *Chem. Eur. J.*, 2010, **16**, 4550.
- [21] C. Sousa, C. de Graaf, A. Rudavskiy, R. Broer, J. Tatchen, M. Etinski and C. M. Marian, *Chem. Eur. J.*, 2013, **19**, 17541.
- [22] C. Roux, J. Zarembowitch, B. Gallois, T. Granier and R. Claude, *Inorg. Chem.*, 1994, **33**, 2273.
- [23] J. S. Kolb, M. D. Thomson, M. Novosel, K. Sénéchal-David, E. Rivière, M.-L. Boillot and H. G. Roskos, *C. R. Chimie*, 2007, **10**, 125.
- [24] M. L. Boillot, J. Zarembowitch and A. Sour, *Spin crossover in Transition Metal Compounds II*, Springer-Verlag, Berlin, 2004, vol. 234, p. 261.
- [25] Y. Hasegawa, S. Kume and H. Nishihara, *Dalton Trans.*, 2009, 280.
- [26] S. Venkataramani, U. Jana, M. Dommaschk, F. D. Sönnichsen, F. Tuczek and R. Herges, *Science*, 2011, **331**, 445.
- [27] H. Ma, J. L. Petersen, V. G. Young, Jr., G. T. Yee and M. P. Jensen, *J. Am. Chem. Soc.*, 2011, **133**, 5644.
- [28] S. Thies, H. Sell, C. Schütt, C. Bornholdt, C. Näther, F. Tuczek and R. Herges, *J. Am. Chem. Soc.*, 2011, **133**, 16243.
- [29] D. Kim, C. Kirmaier and D. Holten, *Chem. Phys.*, 1983, **75**, 305.
- [30] D. Kim and D. Holten, *Chem. Phys. Lett.*, 1983, **98**, 584.

- [31] J. Rodriguez and D. Holten, *J. Chem. Phys.*, 1990, **92**, 5944.
- [32] L. X. Chen, X. Zhang, E. C. Wasinger, K. Attenkofer, G. Jennings, A. Z. Muresan and J. S. Lindsey, *J. Am. Chem. Soc.*, 2007, **129**, 9616.
- [33] A. D. Becke, *Phys. Rev. A*, 1988, **38**, 3098.
- [34] J. P. Perdew, *Phys. Rev. B*, 1986, **33**, 8822.
- [35] Y. Zhao and D. G. Truhlar, *Theor. Chem. Acc.*, 2008, **120**, 215.
- [36] M. J. Frisch, G. W. Trucks, H. B. Schlegel, G. E. Scuseria, M. A. Robb, J. R. Cheeseman, G. Scalmani, V. Barone, B. Mennucci, G. A. Petersson, H. Nakatsuji, M. Caricato, X. Li, H. P. Hratchian, A. F. Izmaylov, J. Bloino, G. Zheng, J. L. Sonnenberg, M. Hada, M. Ehara, K. Toyota, R. Fukuda, J. Hasegawa, M. Ishida, T. Nakajima, Y. Honda, O. Kitao, H. Nakai, T. Vreven, J. A. Montgomery, J. E. Peralta, F. Ogliaro, M. Bearpark, J. J. Heyd, E. Brothers, K. N. Kudin, V. N. Staroverov, R. Kobayashi, J. Normand, K. Raghavachari, A. Rendell, J. C. Burant, S. S. Iyengar, J. Tomasi, M. Cossi, N. Rega, J. M. Millam, M. Klene, J. E. Knox, J. B. Cross, V. Bakken, C. Adamo, J. Jaramillo, R. Gomperts, R. E. Stratmann, O. Yazyev, A. J. Austin, R. Cammi, C. Pomelli, J. W. Ochterski, R. L. Martin, K. Morokuma, V. G. Zakrzewski, G. A. Voth, P. Salvador, J. J. Dannenberg, S. Dapprich, A. D. Daniels, O. Farkas, J. B. Foresman, J. V. Ortiz, J. Cioslowski and D. J. Fox, *Gaussian 09, Revision A.02*, 2009.
- [37] N. Godbout, D. R. Salahub, J. Andzelm and E. Wimmer, *Can. J. Chem.*, 1992, **70**, 560.
- [38] T. H. Dunning and P. J. Hay, *Methods of Electronic Structure Theory*, Plenum, New York, 1977, vol. 3, p. 1.
- [39] A. Klant and G. Schüürmann, *J. Chem. Soc., Perkin Trans. 2*, 1993, 799.
- [40] J. Tomasi, B. Mennucci and R. Cammi, *Chem. Rev.*, 2005, **105**, 2999.
- [41] G. Karlström, R. Lindh, P.-Å. Malmqvist, B. O. Roos, U. Ryde, V. Veryazov, P.-O. Widmark, M. Cossi, B. Schimmelpfennig, P. Neogrady and L. Seijo, *Comput. Mater. Sci.*, 2003, **28**, 222.
- [42] F. Aquilante, L. De Vico, N. Ferré, G. Ghigo, P.-Å. Malmqvist, P. Neogrady, T. B. Pedersen, M. Pitoňák, M. Reiher, B. O. Roos, L. Serrano-Andrés, M. Urban, V. Veryazov and R. Lindh, *J. Comput. Chem.*, 2010, **31**, 224.
- [43] P.-O. Widmark, M. P.-Å. and B. O. Roos, *Theor. Chim. Acta*, 1990, **77**, 291.
- [44] B. O. Roos, R. Lindh, P.-Å. Malmqvist, V. Veryazov and P.-O. Widmark, *J. Phys. Chem. A*, 2004, **108**, 2851–2858.
- [45] B. O. Roos, R. Lindh, P.-A. Malmqvist, V. Veryazov and P.-O. Widmark, *J. Phys. Chem. A*, 2005, **109**, 6575.

- [46] J. P. Perdew, K. Burke and M. Ernzerhof, *Phys. Rev. Lett.*, 1996, **77**, 3865.
- [47] J. P. Perdew, K. Burke and M. Ernzerhof, *Phys. Rev. Lett.*, 1997, **78**, 1396.
- [48] K. Pierloot and S. Vancoillie, *J. Chem. Phys.*, 2006, **125**, 124303.
- [49] B. Ordejón, C. de Graaf and C. Sousa, *J. Am. Chem. Soc.*, 2008, **130**, 13961–13968.
- [50] M. Kepenekian, V. Robert, B. Le Guennic and C. de Graaf, *J. Comput. Chem.*, 2009, **30**, 2327–2333.
- [51] E. V. Brown and G. R. Granneman, *J. Am. Chem. Soc.*, 1975, **97**, 621.
- [52] M. Gouterman, *J. Chem. Phys.*, 1959, **30**, 1139.
- [53] M. Gouterman, G. H. Wagnière and L. C. Snyder, *J. Mol. Spectrosc.*, 1963, **11**, 108.
- [54] C. Weiss, H. Kobayashi and M. Gouterman, *J. Mol. Spectrosc.*, 1965, **16**, 415.
- [55] L. Serrano-Andrés, M. Merchán, M. Rubio and B. O. Roos, *Chem. Phys. Lett.*, 1998, **295**, 195.